Vol. 16, No. 1 (2017) 131-146
Revista Mexicana de Ingeniería Química

HIGH-PRESSURE HOMOGENIZATION AND MALTODEXTRINS MIXTURES TO MICROENCAPSULATE VANILLA (*Vanilla planifolia*) EXTRACT THROUGH FREEZE-DRYING

HOMOGENEIZACIÓN A ALTA PRESIÓN Y MEZCLAS DE MALTODEXTRINAS PARA MICROENCAPSULAR EXTRACTO DE VAINILLA (*Vanilla planifolia*) MEDIANTE LIOFILIZACIÓN

I.O. Ocampo-Salinas[1], A. Jiménez-Aparicio[2], M.J. Perea-Flores[3], A. Tapia-Ochoategui[1], M.P. Salgado-Cruz[1], C. Jiménez-Martínez[1], D.I. Téllez-Medina[1]*, G. Dávila-Ortiz[1]

[1] *Departamento de Ingeniería Bioquímica, Escuela Nacional de Ciencias Biológicas, Instituto Politécnico Nacional, Unidad Profesional Adolfo López Mateos, Av. Wilfrido Massieu Esq. Cda. Manuel Stampa S/N, C.P.07738 Delegación Gustavo A. Madero, Ciudad de México, México.*

[2]*Instituto Politécnico Nacional-Centro de Desarrollo de Productos Bióticos. Carretera Yautepec-Jojutla, Km 6.8, San Isidro, Yautepec, Morelos, México CP 62730.*

[3]*Centro de Nanociencias y Micro y Nanotecnologías. Instituto Politécnico Nacional, calle Luis Enrique Erro s/n Unidad Profesional Adolfo López Mateos. Col. Zacatenco. C. P. 07738. Ciudad de México, México*

Received October 16, 2016; Accepted December 21, 2016

Abstract Microfluidization followed by encapsulation through freeze-drying was performed in order to assess the effect of high pressure homogenization (70 MPa, one and two cycles) and the coating material composed of maltodextrins (MD) mixtures with different dextrose equivalent (DE) values, DE 10 (MD10) and DE 20 (MD20) at 10% (w/w) total solids content, on the feasibility of concentrated vanilla extract (VE) encapsulation. The rheology of five different formulations was determined before microfluidization, while particle size was determined after such processing stage. After freeze-drying, it was determined the encapsulation efficiency (%EE), also the microcapsules were analyzed by laser scanning confocal microscopy, X-ray diffraction and differential scanning calorimetry. The Herschel-Bulkley and Ostwald-de Waele models were found to adequately describe the rheology of formulations so that the consistency coefficient increased with content of MD10. The particle size was markedly lowest for the formulation containing only MD10; this formulation presented a semi-crystalline X-ray pattern while formulations containing MD20 indicated an amorphous pattern and glass transition temperature in the order of 65 °C. MD20-MD10 mixtures 90:10 and 95:05 reported the highest %EE after one microfluidization cycle. In the present work, it was possible to obtain matrix-type microcapsules of VE with high %EE (> 95%).

Keywords: vanillin, maltodextrins, microfluidization, encapsulation efficiency, microstructure.

Resumen

Microfluidización seguida de encapsulación mediante liofilización fue realizada para evaluar el efecto de la homogeneización por altas presiones (70 MPa, 1 y 2 ciclos) y del material de pared compuesto por mezclas de maltodextrinas (MD) con diferente equivalente de dextrosa (DE), DE 10 (MD10) y DE 20 (MD20), con 10% (p/p) de sólidos totales, sobre la factibilidad de encapsular extracto concentrado de vainilla (VE). Antes de microfluidizar, se determinó la reología de cinco formulaciones diferentes; el tamaño de partícula fue determinado después de dicha etapa. Después de liofilizar, se determinó la eficiencia de encapsulación (%EE); las microcápsulas fueron analizadas mediante microscopía confocal de barrido láser, difracción de rayos X, y calorimetría diferencial de barrido. Los modelos Herschel-Bulkley y Ostwald-de Waele describieron adecuadamente la reología de las formulaciones; el coeficiente de consistencia aumentó con el contenido de MD10. La formulación con únicamente MD10 presentó el tamaño de partícula menor y patrón de rayos X semicristalino; las formulaciones con MD20 exhibieron un patrón amorfo y temperatura de transición vítrea cercana a 65 °C. Las mezclas MD20-MD10 90:10 y 95:05 reportaron la %EE mayor después de un ciclo de microfluidización. En el presente estudio fue posible obtener microcápsulas de VE con alta %EE (>95%).

Palabras clave: vainillina, maltodextrinas, microfluidización, eficiencia de encapsulación, microestructura.

* *Corresponding author. E-mail*: darioiker@gmail.com

1 Introduction

According to FDA, vanilla extract (VE) must contain at least the sapid and odorous principles extracted by an aqueous alcohol solution of not less than 35% ethyl alcohol. A single fold of VE contains the extractable material from 100 g vanilla beans/L of solvent. Natural vanilla flavor is a complex mixture of volatile substances and over 170 volatile components have been identified in natural extracts (Sostaric *et al*., 2000), but vanillin (4-hydroxy-3-methoxybenzaldehyde) is the principal component (Gu *et al*., 2012; Sharma *et al*., 2006); however, green vanilla beans lack in flavor and aroma, so a curing process is necessary for the formation of such volatile compounds responsible for aroma (Tapia-Ochoategui *et al*., 2011).

The sensory perception of vanilla extract can be changed as a result of oxidation, chemical interactions or volatilization of its labile components. In order to minimize the harm of these negative processes and to limit aroma degradation or loss during processing, microencapsulation is used in flavor industry to entrap liquid flavoring substances, such as essential oils, aroma and flavor mixtures in a matrix of wall materials (Jun-xia *et al*., 2011; Madene *et al*., 2006; Milanovic *et al*., 2010).

The selection of wall material is an important step for the success of the microencapsulation process. The encapsulation wall system is made of compounds that have hydrophilic and/or hydrophobic groups, which create a network-like structure and whose selection depends on the core material and desired characteristics of the microcapsules. Typical shell materials for flavor encapsulation include the maltodextrins (MD) (Baranauskiene *et al*., 2007; Quintanilla-Carvajal *et al*., 2011; da Costa *et al*., 2012).

MD are starch hydrolysates that have low bulk density, resistance to caking, blandness, excellent mouthfeel, film forming, binding, nutritive value, oxygen barrier and surface sheen properties (Avaltroni *et al*., 2004; Sánchez *et al*., 2013) with a dextrose equivalent (DE) equal or less than 20. The DE is a measure of the reducing power as compared to D-glucose on a dry-weight basis: the higher DE the greater extent of starch hydrolysis; DE is an inverse scale of the degree of polymerization (DP) of anhydrous glucose units. Maltodextrins with different DE value have different physicochemical properties (Dokic *et al*., 2004; Wang *et al*., 2012).

Soottitantawat *et al*. (2005) have reported the importance of modifying the droplet size of an emulsion before being subjected to a drying process, in order to improve encapsulation efficiency. Finest emulsions are usually produced using high-energy methods, such as microfluidization (Qian and McClements, 2011; Flores-Miranda *et al*., 2015; Ochoa *et al*., 2016; Domínguez-Hernández *et al*., 2016). Microfluidization has been used extensively for particle deagglomeration, dispersion and size reduction; such process takes place when the fluid enters in microchannels of two different interaction chambers (Y and Z), thus exposing uniformly the liquids to high shear stresses. The different interaction chambers correspond to distinct geometric configurations of the homogenization valves used for microfluidization processing, the names 'Y' and 'Z' refer to the conduit conformation in the inner part of such valves (Ocampo-Salinas *et al*., 2016). The process pressure and the channel geometry control the velocities inside the channels, and therefore the energy dissipation. In general, inertial forces in turbulent flow along with cavitation are predominantly responsible for disintegration of agglomerates (Patravale *et al*., 2004; Jafari *et al*., 2007a; Panagiotou *et al*., 2008; Siqueira *et al*., 2010; Yang *et al*., 2012; Cano-Sarmiento *et al*., 2014; Monroy-Villagrana *et al*., 2014).

The huge market demand and high price of natural vanilla extract have provided an economic incentive to enhance poor quality vanilla extract with synthetic vanillin (Hoffman and Zapf, 2011; Sinha *et al*., 2008). Hence, it is also important the ability to process these extracts without adulterating and to develop a value-added product; however, due to lack of information about the effect of high pressure homogenization on vanilla extract encapsulation it was aimed to explore the preparation of microcapsules of vanilla extract in maltodextrin mixtures through microfluidization followed by freeze-drying. The main purpose of the present work was to observe the effect of homogenization by microfluidization and the coating material formulation composed of maltodextrins mixtures on the efficiency of vanilla extract encapsulation performed by freeze-drying.

2 Materials and methods

2.1 Material

Cured vanilla beans vacuum packed (provided by Consejo Nacional de Productores Vainilleros AC from

Veracruz, Mexico), Vanillin (reagent grade, Sigma-Aldrich, Germany), MD DE 20 powder (MD 20, Food Supplements, Naucalpan, Mexico), MD DE 10 powder (MD 10, Ingredion, Mexico), absolute ethanol (analytical grade). Water used was type I (MilliQ, Ireland).

2.2 Experimental methods

2.2.1 Preparation of vanilla extract

The extract was prepared through a modification of Ranadive (1992) method: 100 g of cured vanilla beans were cut without crushing and macerated in 700 mL aqueous ethanol (40% v/v) for one week at 25°C. The mixture was stirred, filtered, washed with 40% ethanol up to the total volume reached 1 L (single fold VE) and concentrated by vacuum evaporation (Buchi, Switzerland) at 45°C (Jadeja *et al*., 2012). Total vanillin in concentrated VE was determined by the AOAC method 966.12 (AOAC, 2005) using a spectrophotometer (Boeco S-22, Germany) at 348 nm and was expressed as mg vanillin/mL of extract. The AOAC method indicated the use of a calibration curve which was prepared from aqueous solutions of vanillin and NaOH 0.1 N. The amount of VE used in further analyses was based on the concentration of vanillin found through the method detailed here.

2.2.2 Preparation of homogenized formulations

Formulations were prepared by addition of MD 10 (formulation A) or MD 20 (formulation E) and their blends in a ratio E:A of 85:15 (formulation B), 90:10 (formulation C) and 95:5 (formulation D) w/w, to obtain 10% w/w total solids content. For each formulation 16.4 mL of VE (about 40 mg of total vanillin) were added and adjusted with water up to 300 g of weight; this represented a 1:60 active-wall material ratio. All formulations were mixed by using an UltraTurrax T25 (Janke and Kundel Ika-Labortechnik, Germany) operating at 13500 rpm for about 1 min to obtain the so-called predispersions.

2.2.3 Rheology of predispersions

The rheology of the five different formulations was determined at 25 °C by using a rotational viscometer Roto-Visco1, HAAKE (Thermo Fischer Scientific, Germany) with an Z31 spindle working at 0-200 s^{-1} shear-rate range for 120 s at 25 °C (constant temperature maintained by a HAAKE-DC30 unit) (Marcotte *et al*., 2001; Nielsen 2003; Dokic *et al*., 2004). Sample volume for the tests was 52 mL. Stress-deformation curves for all formulations (A-E) were obtained in order to identify the best rheology model for matching the behavior of maltodextrins mixtures. The model parameters were obtained by non-linear regression using the software RheoWin Data Manager 4.0 (Thermo Fischer Scientific), from 5 different sets of points to each sample.

2.2.4 Microfuidization of predispersions

Each of the above predispersions were passed through the microfluidization equipment (Microfluidics, M-110, Newton, MA, USA) in order to obtain a dispersion from each formulation with one and two cycles at a pressure of 70 MPa.

2.2.5 Determination of particle size

The average particle size of the microfluidized dispersions was determined by dynamic light scattering using a Zetasizer Nano-ZS90 (Malvern Instruments, Worcestershire, UK) at a fixed detector angle of 90°. To minimize multiple scattering effects, prior to each measurement, dispersions were diluted using a 3:500 dilution factor. Results were described as accumulated mean diameter (reported in nm) for particle size.

2.2.6 Freeze-drying

After microfluidization, weighed amounts of the formulations were placed into amber vials, frozen at -70 °C for 24 h and freeze-dried (Virtis, consol 255L, France) at -40°C and 0.3 mbar. After freeze-drying each vial was weighed. All freeze-dried samples, obtained from the corresponding formulation after 1 cycle (A_{FD1}, B_{FD1}, C_{FD1}, D_{FD1} and E_{FD1}) and 2 cycles (A_{FD2}, B_{FD2}, C_{FD2}, D_{FD2} and E_{FD2}) of microfluidization were stored into sealed desiccators at 25°C.

2.2.7 Confocal laser scanning microscopy

For confocal laser scanning microscopy (CLSM) analysis each freeze dried sample was mounted on a glass slide and observed under a multiphotonic microscopy (LSM 710 NL0, Carl Zeiss, Germany) with a 20X objective. The laser excitation wavelengths were 405, 488, 561 and 633 nm. This capture mode used a spectral imaging technique that automatically outputs separated channels of the multiple labeled samples; this is based on an

optimized algorithm (linear mathematical algorithm for spectral unmixing), which allowed the separation of the overlapping channels from emission spectra (Hernández-Hernández *et al*., 2014). This microscopy was equipped with a spectral channel used to detect autofluorescence signals such as vanilla derivatives (Yang *et al*., 2014). The components were compared with reference spectra (Dickinson *et al*., 2001) (autofluorescence of individual materials: M10, MD20 and VE) to confirm their fluorescence intensity. The measurements of the fluorescence intensity were performed using the software ZEN 2010 (Carl Zeiss, Germany). The z-stack images (it allows 3D reconstruction) were obtained to the top surface of ungrounded samples and were saved in RGB format with a size of 1797x1133 pixels.

2.2.8 X-Ray diffraction

Determination of possible crystallinity of raw wall material (MD10 and MD20) and freeze dried samples was performed by X-Ray diffraction, in a diffractometer (Rigaku, model miniflex 600, Japan). The radiation used was generated by a CuKα filter with a wavelength of 15.4 nm at 40 kV and 15 mA current. Samples were scanned from 2 to 60° (2θ) at 4 °/min scanning rate.

2.2.9 Differential scanning calorimetry (DSC)

A differential scanning calorimeter (Diamond DSC, Perkin-Elmer Precisely) with Pyris operation software was used for the determination of glass transition temperature (Tg) and change in heat capacity (ΔCp) of the microcapsules obtained after the freeze-drying stage. The calorimeter was equipped with an intercooler (2P, Perkin-Elmer) and nitrogen purge gas. Before the analysis, the equipment was calibrated with Indium (156.6 °C m.p.). For the Tg determination, it was used a modified version of the method proposed by Pérez *et al*. (2014), for determining the Tg in samples of cassava starch mixed with corn oil with physical aging: 10 mg samples were contained into hermetically sealed stainless steel pans, cooled to -20 °C and then heated to 110°C at 10 °C/min. A second heating scan took place for each sample under the same conditions. The first heating was performed to eliminate any aging effect during storage whereas the second one aimed to determine the Tg and ΔCp. The water activity of the samples before the analysis was determined with an Aqualab 4TE (Decagon Devices, USA) and ranged 0.353-0.375.

2.2.10 Determination of encapsulation efficiency (%EE) of vanillin

It was used the method of Rodríguez *et al*. (2013) after modifications. Vanillin on surface of particles was extracted in absolute ethanol. Samples of 0.1 g of grounded freeze dried microcapsules were mixed with 10 mL of absolute ethanol in a sealed beaker and agitated with a magnetic stirrer for 90 min. The microcapsules were filtered through Whatman No. 6 paper. The absorbance was read using a spectrophotometer (Boeco S-22, Germany) at 277 nm. The encapsulation efficiency (%EE) of encapsulated VE was calculated following Eq. (1).

$$\%EE = \frac{\text{Total add vanillin -Vanillin on surface}}{\text{Total add vanillin}} \times 100 \quad (1)$$

As reference blank, for each sample it was used a filtrated washing ethanolic solution from a dispersion subjected to the same conditions of microfluidization and freeze-drying than the sample with the respective ratio of MD10:MD20, but without VE. The rest of each sample after washing with ethanol was redispersed in water and, afterwards, the concentration of the inner content of vanillin was determined as for the VE in section 2.2.1.

2.2.11 Statistical analysis

The vanillin mean concentration in the extracts and the standard error were calculated. For the rest of the analyzed parameters a two-way analysis of variance was carried out and multiple comparison Holm-Sidak test was used. For the normalization of the data, a treatment of radial conversion was carried out only for the %EE values (Bromiley and Thacker, 2002). Each sample was tested by triplicate. Minitab 17 (Minitab Inc. USA) software was used. In all cases it was assumed a significance level of $2\alpha = 0.05$.

3 Results and discussion

3.1 Vanilla extract

The one fold vanilla extract obtained had a vanillin content of 1.46 mg/mL, such concentration could be compared to that of regulated commercially available natural vanilla extracts (about 1.0 g vanillin/ L extract) Sinha *et al*., (2008). However according to Ranadive (2011) the vanilla extract obtained in the current work had lower concentration than that of high quality extracts (≈2 mg/mL). As expected, the concentration

of vanillin raised to 2.43 mg/mL in VE according to the quantity of ethanol evaporated.

3.2 Rheological analysis

Accordingly to the stress-deformation curves observed (data not shown) and analyzed through the software of the viscometer, strictly, all samples exhibited a flow behavior explained by the Herschel-Bulkley model ($R^2 > 0.99$), specifically a shear-thickening behavior with a low yield shear-stress; nonetheless, the Ostwald-de Waele (power law) and Newton models also reported high determination coefficients ($R^2 > 0.985$ and $R^2 > 0.98$, respectively). Moreover, given the low values of the yield shear-stress (in the order of 0.18 Pa) and the statistical similarity in the value of this parameter among the different formulations, the Ostwald-de Waele (Eq. 2) model was used to compare the rheology of the different formulations (see Table 1):

$$\sigma = K\dot{\gamma}^n \tag{2}$$

Where σ is the shear stress, $\dot{\gamma}$ is the shear rate, K is the consistency coefficient and n is the flow behavior index that describes the flow behavior of the fluid as shear-thinning ($n < 1$) or shear-thickening ($n > 1$) (Marcotte *et al*., 2001).

Table 1 shows the consistency coefficient and the flow behavior index of analyzed maltodextrins mixtures. The consistency coefficient, that showed values between 12.20 and 6.69 mPa·s^n, was reduced as the ratio of MD10 was diminished, but from formulation A to formulation B an important viscosity drop was observed since MD10 proportion was decreased in great level. Besides, the relationship between the increase in the proportion of MD10 and the rise of the viscosity was linear with a value of R^2=0.9973. The decrease in viscosity from formulation A to formulation E might resulted in such trend because the short-chain glucose unit fractions of maltodextrin are less efficient for increasing the resistance to flow (Udomrati *et al*., 2013). The difference in consistency coefficients between MD10, MD20 and their mixtures was in agreement with Dokic *et al*., (1998) who reported that the viscosity of maltodextrin solutions depends on DE value, so that the higher DE value the lower the viscosity.

Unlike the present study, a number of works (Dokic *et al*., 1998; Avaltroni *et al*., 2004; Dokic *et al*., 2004; Adhikari *et al*., 2007) have reported a Newtonian behavior for maltodextrins dispersions with distinct DE at various concentrations; however, Sikora *et al*. (2002) reported that suspensions of alumina mixed with maltodextrin corn at 1% (wt.) fitted the Herschel-Bulkley model, whilst Chetana *et al*. (2004) worked with MD16 and polydextrose mixtures and found a Herschel-Bulkley fitting and a shear-stress in the order of 0.19 Pa; nevertheless, in both works it was observed a shear-thinning flow behavior although they corresponded to a total content of solids larger than 35%.

In the current work the flow behavior index values were from 1.024 to 1.097 (dimensionless) indicating that all dispersions expressed a slightly shear-thickening behavior which decreased with lower MD10 concentration; hence, dispersions tended to enhance their shear-thickening behavior with higher amount of MD20. Udomrati *et al*. (2013) reported index behavior values slightly greater than 1, for maltodextrin solutions ranging 5-35% w/w total solids content. A shear-thickening behavior was reported by Wang *et al*. (2011) in diluted dispersions ≤ 10% of waxy maize starch; they assumed that such property was conditioned by a shear-resistant structure of dissolved amylopectins in the continuous phase, so that given the flow behavior indexes close to 1 obtained in the current work, a similar effect of formation of a weak structure could be obtained due to physical interaction of soluble solids fromVE and the different molecular mass chains of saccharides in the samples.

Table 1. Viscosity results according to Ostwald-de Waele model (Eq. 1).

Formulation	K (mPa·s^n)*	n (dimensionless)	R^2
A	12.20 ± 0.13	1.024±0.013	0.9896
B	7.37 ± 0.08	1.088±0.009	0.9892
C	7.32 ± 0.07	1.089±0.008	0.9898
D	6.73 ± 0.08	1.093±0.009	0.9874
E	6.69 ± 0.06	1.097±0.007	0.9902

*mean ± standard error values from 5 measurements.

Table 2. Particle size distributions after 1 and 2 microfluidization cycles.

Formulation	1 cycle d (nm)	2 cycles d (nm)
A	177.43^{a} ±9.88	208.27^{a} ±17.12
B	622.33^{b} ±4.20	$483.07^{b,c}$ ±16.76
C	506.63^{c} ±21.62	561.10^{c} ±34.11
D	$576.17^{b,c}$ ±31.19	420.90^{b} ±26.70
E	709.10^{d} ±21.92	555.53^{c} ±8.61

Equal letters between lines indicate significant statistical similarity. Significance level was $2\alpha = 0.05$.

Table 3. ΔC_p and Tg of samples from dispersions after 1 microfluidization cycle.

Sample	ΔCp J/g ºC	Tg °C
A_{FD1}	ND*	ND*
B_{FD1}	0.173	66.72
C_{FD1}	0.425	64.55
D_{FD1}	0.547	65.16
E_{FD1}	0.365	65.73

*The DSC software did not detect a clear value for these parameters

3.3 Particle size

As indicated in the corresponding methodology section (2.2.5), the samples required to be diluted up to obtain a suitable scattering intensity. Nevertheless, in order to investigate how dilution affects the size distribution of our samples, few tests were performed by varying the dilution factor which reported that from the dilution 3:500 the polydispersity index did not change as the dilution increased. The dilution ratio was not far in Ji *et al*. (2015) when using the same analysis equipment and under similar conditions.

In Table 2, the particle size distribution of all samples after 1 and 2 microfluidization cycles is depicted. After 1 microfluidization cycle, with only MD10 (formulation A), it was caused a smaller particle size up to a diameter (d) about 177 nm, while on the opposite using MD20 alone it was obtained the largest particle diameter. The trend followed by the rest of the samples was associated to the content of MD10 so that a smaller particle size was obtained as the amount of MD10 increased. However, the result showed by formulation B did not followed such trend since its particle size was not lower than the formulation D and E. Furthermore, it is necessary to note that the shear-thickening behavior might induce particle aggregation (Wang *et al*., 2011) and the MD20-MD10 ratio of sample B probably enhanced this sample to present a greater particle size.

Regarding the samples after 2 microfluidization cycles, also formulation A showed the smallest diameter among the samples; however, formulation C presented the largest particle diameter. It was interesting that, except sample A, there was no a clear relation between MD10 content and particle size, although when comparing the samples it was evident that the consequence of an extra microfluidization cycle was a narrower particle size distribution, probably because a second microfluidization cycle improved the homogenization efficiency; on this matter, Jafari *et al*. (2007b) concluded that 1 and 2 microfluidization cycles and moderate pressures were optimum for producing nanoemulsions of D-limonene with a narrow size distribution.

The consistency coefficient showed by formulation A seemed to affect its particle diameter, probably because the addition of polymers that increase dispersion viscosity improves the efficiency of particle size reduction (Patravale *et al*., 2004). In emulsions technology an increase of continuous phase viscosity usually decreases the droplet diameter (Qian and McClements, 2011) since it slows the movement of the drops (Jafari *et al*., 2007a).

Formulation A exhibited a bimodal particle size with a polydispersity index (PI) of 0.50 after 1 and 0.4 after 2 microfluidization cycles. Assuming that the statistical parameter called PI allows to infer about the dispersion in sample data, the results indicated an effect in this parameter caused by the application of different microfluidization cycles, as observed for samples B, D and E. Such behavior might be explained

by the coexistence of low-molecular weight chains with chains of higher molecular weight, as in the case of MD10, causing an increase in dispersity. The rest of formulations showed a monomodal PIbetween 0.14 and 0.24 for 1 microfluidization cycle and 0.22 and 0.29 for 2 microfluidization cycles.

3.4 Confocal laser scanning microscopy

Figure 1(1) presents the reference spectra for wall material (MD10 and MD20) and the VE without microfluidization and freeze-drying process. For the detection of the individual signals in the samples three maximum peaks of the reference material were used, with wavelengths of 461 nm for MD20 and MD10 and 500 nm for VE; when the 3 signals were present, the maximum for MD10 was at 500 nm and for VE was at 597 nm.

After freeze-drying solid agglomerates with irregular shape and porous structures were obtained, typical of the use of such process (Fang and Bhandari, 2010).The fluorescence signals of the images obtained by CLSM from all analyzed samples, allowed to detect that the VE was entrapped within the wall material in an important quantity, but the relation of the coating material may affect the arrangement of the matrix. Figure 1(2) shows the z-stack images of fluorescence signals from the components corresponding to samples A_{FD1} (1.2a) and A_{FD2} (1.2b) and E_{FD1} (1.2c) and E_{FD2} (1.2d).

In samples A_{FD1} and A_{FD2}, according to the images, MD10 formed a homogeneous and continuous matrix-type thick layer (blue areas) coating the VE (green areas). The sample A_{FD2} seems to be formed by a laminated structure of thick layers. It was interesting to note, in both samples, the absence of VE on the surface of the crust; and this was more notorious in sample A_{FD1}.

In the case of samples E_{FD1} and E_{FD2}, in the former the VE quantity (green areas) was spread into MD20 (red areas) in a heterogeneous way; however, in the latter, even though it acquired a similar heterogeneous distribution apparently this was more uniform. Both samples formed matrix-type microcapsules so that thin layers covering the VE were observed. Particularly, sample E_{FD2} showed laminated compact structures between the active principle and the wall material, probably because a second microfluidization cycle improved the homogenization efficiency.

In agreement with the current work, Harnkarnsujarit *et al.* (2012) reported that high molecular weight carbohydrates tend to form thicker walls while carbohydrates with shorter chains formed thinner walls. This explains the structures observed in the current work, since the coating material in samples A_{FD1} and A_{FD2} had saccharides with higher molecular weight than samples E_{FD1} and E_{FD2}.

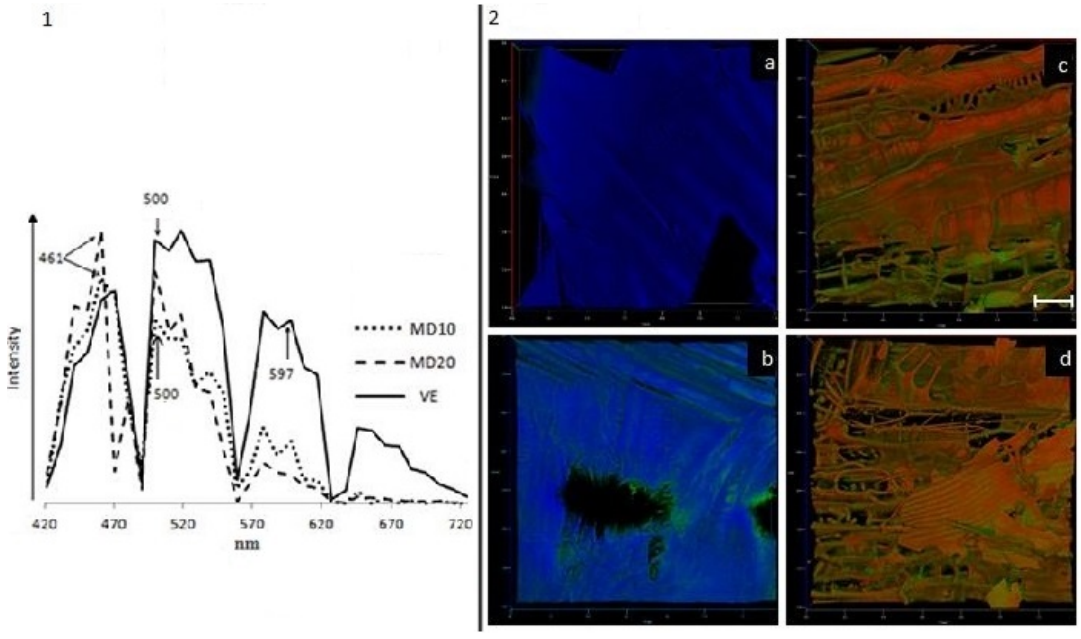

Figure 1. 1. Characterization of autofluorescence emission profiles of materials; 2. 3D reconstruction of the

microstructure of freeze-dried samples a: A_{FD1}, b: A_{FD2} c: E_{FD1}, d: E_{FD2} (blue: MD10; red: MD20; green: VE). 20X objective. Scale refers to 200 μm.

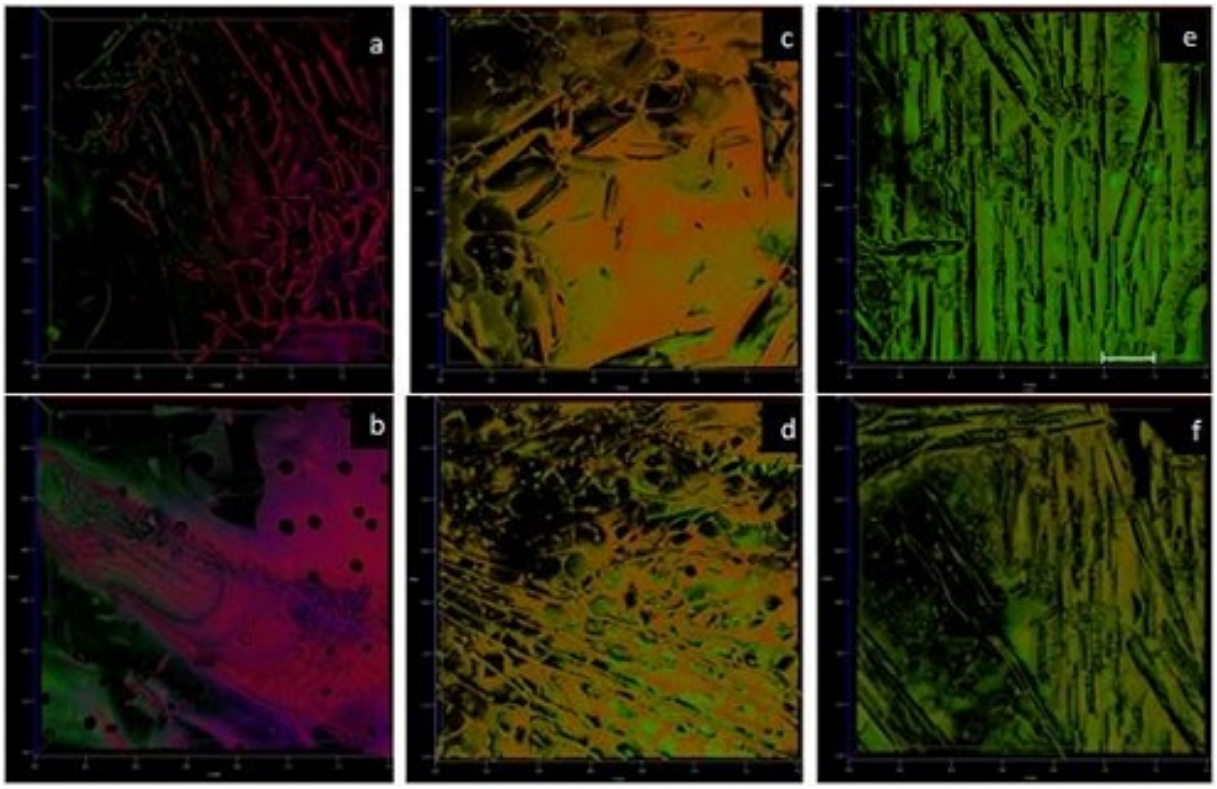

Figure 2. 3D reconstruction image of microstructure of freeze-dried samples; a: B_{FD1}, b: B_{FD2}, c: C_{FD1}, d: C_{FD2}, e: D_{FD1}, f: D_{FD2} (blue: MD10, red: MD20, green: ECV). 20X objective. Scale refers to 200 μm.

Regarding formulations with MD20-MD10 mixtures, in the samples C_{FD1} (Figure 2c), C_{FD2} (Figure 2d), D_{FD1} (Figure 2e) and D_{FD2} (Figure 2f) probably due to the lower amount of MD10, the CLSM could not identify the fluorescence signal of MD10. The images of the samples mentioned above showed that the VE had a less heterogeneous distribution into the coating matrix, which may indicate that the active principle was more efficiently entrapped than in the case of E_{FD1} and E_{FD2} samples. This is an important observation because similar structures would be expected in C_{FD1}, C_{FD2}, D_{FD1}, D_{FD2}, E_{FD1} and E_{FD2} samples, given MD20 was the main coating material; hence, the MD10 content was determinant in the microstructure of the capsules obtained by freeze-drying.

The images of samples B_{FD1} (Figure 2a) and B_{FD2} (Figure 2b) showed a third fluorescence signal (blue area); an increase in the proportion of MD10 in the formulation B could enable the equipment for detecting the fluorescence intensity of MD10, so that the mixture of wall materials (purple areas) was observed; however, in these samples the scarce presence of VE on the surface was noticeable, similarly to what was observed from samples A_{FD1} and A_{FD2}.

3.5 X ray diffraction

Figure 3 (Left) shows the X-ray diffraction patterns of raw MD10 and MD20 and samples A_{FD1}, A_{FD2}, E_{FD1} and E_{FD2}. Most of the signals in the diffraction pattern of samples A_{FD1} and A_{FD2} match the ones reported for crystallized corn starch (Zobel, 1964), as expected, given the origin (informed by the supplier) of the MD used in this work. Both samples, A_{FD1} and A_{FD2} (Figure 3a, bottom), revealed certain degree of crystallinity showing similar reflection angles at 17.05°, 19.48° and 22.02° for A_{FD1} and 17.09°, 19.65° and 22.07° for A_{FD2}, which means that a

second cycle of microfluidization did not change the diffraction pattern; however, apparently the peak intensity increased and even peaks about 19° and 22° were well defined as compared to the respective peaks of A_{FD1}.

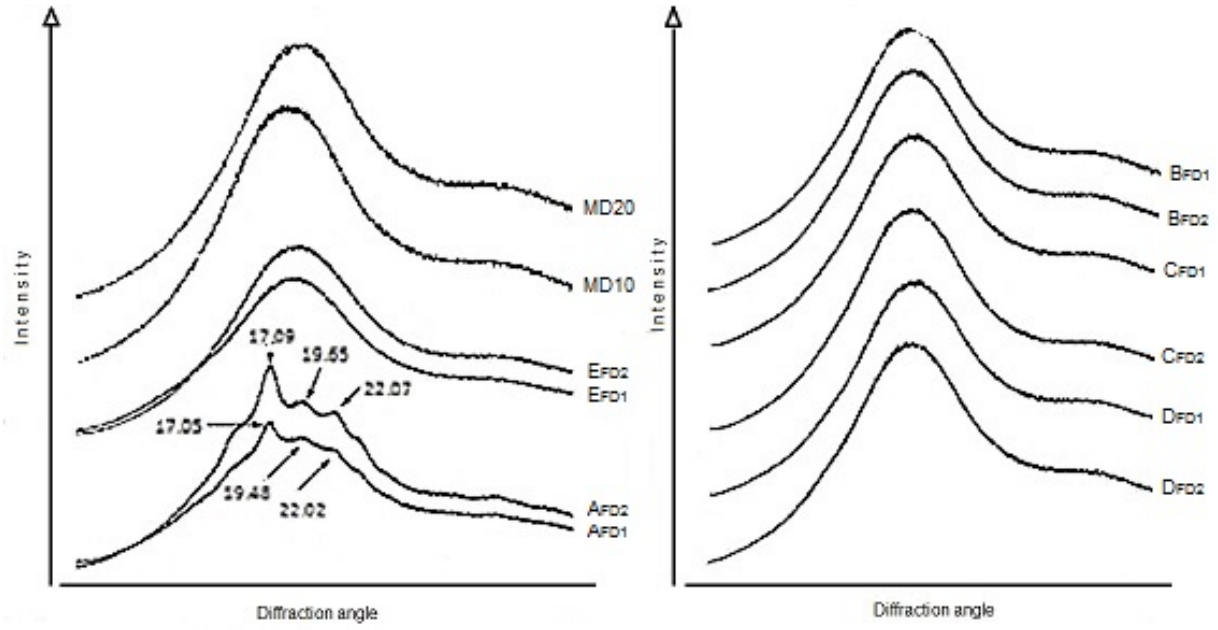

Figure 3. X-ray diffraction patterns of raw material and freeze-dried dispersions. Left, diffraction patterns of raw MD10 and MD20, and dispersion of maltodextrins E_{FD1} (MD20-1 cycle), E_{FD2} (MD20-2 cycles), A_{FD2} (MD10-1 cycle) and A_{FD1} (MD10-2 cycles). Right, diffraction patterns of maltodextrins mixtures B_{FD1}, B_{FD2}, C_{FD1}, C_{FD2}, D_{FD1} and D_{FD2}.

Unlike the amorphous state, crystallization could be a drawback in encapsulation technology, because systems with crystallized saccharides are less capable of retaining the encapsulated volatiles (Buera *et al*., 2005); hence, it is possible that with samples A_{FD1} and A_{FD2}, such negative aspect could affect their encapsulation properties.

Accordingly with the current work, Jeon *et al*., (2003) observed a crystalline pattern in freeze-dried native high amylose maize starch gel (10% solids) with similar diffraction angles as our data (17.1, 20.2 and 22.5°), they indicated that the sample displayed the typical B-type diffraction patterns for retrograded starch and explained that crystal structure was mainly formed during the freezing process. Given that the X-ray pattern of raw MD10 (Figure 3 left, top) showed an amorphous structure, it is probably that during the freezing process, the MD10 of A_{FD1} and A_{FD2} samples acquired a B-type semi-crystalline structure.

Microcapsules of samples E_{FD1} and E_{FD2}, with only MD20 (Figure 3 Left, middle), were found to be amorphous, same as raw MD20 (Figure 3 Left, top). Probably because MD20 was the main material in the microcapsules from samples B_{FD1}, B_{FD2}, C_{FD1}, C_{FD2}, these acquired a similar structure (Figure 3, Right) to E samples. It seems that saccharides chains of lower molecular weight, as in the case of MD20, were not prone to form crystalline or semi-crystalline structures; accordingly, Corveleyn and Remon (1996) reported an amorphous structure after freeze-drying process for maltodextrin with DE similar to that of the MD20 used in the current work.

3.6 Differential scanning calorimetry

The Tg and glass transition ΔC_p of the capsules obtained from samples subjected to 1 microfluidization cycle are shown in Table 3. The Tg of each sample was determined from the middle point of the heat capacity change during the second heating. The relatively high value of Tg showed by the microcapsules seems to be in agreement with the practice of adding high molecular weight

carbohydrates (such as MD) in order to generate compact and firm appearance. A high Tg value indicates low susceptibility to develop microstructure changes during freeze-drying (Galmarini *et al*., 2009).

No clear change on heat flow due to changes in ΔC_p was seen for sample A_{FD1} with a second heating; this agrees with Nurhadi *et al*. (2016), they reported that a exothermic transition for freeze-dried maltodextrins DE10 (0.33-0.65 aw) due to glass transition disappeared with a second heating. Sample A_{FD1} contained only MD10 (as showed the X-ray diffraction analysis, was able to acquire some crystallinity degree) as wall material. In granular starch model with crystallinity degree, only the mobile amorphous phase contributes to the change of ΔC_p during Tg determination by DSC (Liu *et al*., 2006); however, the absence of a visible glass transition ΔC_p could be due to crystalline regions acting as physical cross links that impose restriction to segmental motion in the surrounding amorphous phase and induce changes in the thermal properties of the amorphous material and thus suppress ΔC_p. For example in polycarbonate, with a degree of crystallinity as low as 23%, there is no detectable ΔC_p (Biliaderis *et al*., 1986). With respect to Tg of sample A_{FD1}, a polymer with some degree of cristallinity, such temperature is not clearly independent of the crystalline melting temperature (Liu *et al*., 2006).

Accordingly to the ΔC_p results, and the CLSM images, it was observed that the MD20-MD10 ratio of the samples might influence the structure of microcapsules. With respect to the sample B_{FD1}, this sample presented the lowest ΔC_p, apparently such value was related to the MD10 content since this sample contained the highest amount of this MD. The presence of certain degree of crystallinity tends to decrease the glass transition ΔC_p (Menczel *et al*., 2009). For determining crystallinity in starch, the X ray diffraction is less sensitive to structures packaged irregularly, shaped aggregates of small chain or individual helices isolated (Wang *et al*., 2015); thus, that could explain why the X-ray analysis did not detect the cristallinity degree of the MD10 present in sample B_{FD1} (15% w/w).

However, the samples C_{FD1} and D_{FD1}, showed even higher ΔC_p values than sample E_{FD1} (containing only MD20). This indicates that the effect of decreasing the sample ΔC_p may be determined not only by the semi-crystalline nature of MD10 but also by the MD20-MD10 ratio. It seems that the amount of MD10 present in B was high enough to diminish the glass transition ΔC_p, whereas in the case of C_{FD1} and D_{FD2} samples, the MD10 content was too low to exert such effect.

3.7 Encapsulation efficiency

Results indicated that only 1 microfluidization cycle is enough to obtain microcapsules with high %EE of VE. Samples C_{FD1} and D_{FD1}, which were blends containing 10 and 5% MD10, respectively, showed a %EE significantly higher than the rest of the samples subjected to 1 cycle (Table 4). The statistical analysis indicated that the application of two cycles of microfluidization did not reduce significantly the %EE in the samples, although the sample A_{FD2} showed a significant reduction in this parameter with respect to sample A_{FD1}. The experimental procedure followed in the current work generated results comparable to those reported (94.2%) by Yang *et al*. (2014) when they obtained microcapsules of vanilla oil by complex coacervation and freeze-drying and using chitosan and gum Arabic as wall material.

The relatively high values of %EE obtained in the current work were due probably to the affinity between VE and MD10 and MD20. Goubet *et al*., (1998) suggested that the solubility of the active compound plays an important role during the retention of volatiles in carbohydrates matrices during freeze-drying; a higher polarity of an odorant principle results in that such volatile diffuses more easily through the

Table 4. Encapsulation efficiency of freeze dried dispersions obtained from different microfluidization cycles.

Formulation	1 cycle %EE	2 cycles %EE
A	93.92^{a} ±0.41	85.38^{a} ±1.80
B	93.48^{a} ±0.28	93.02^{b} ±0.42
C	98.41^{b} ±0.35	97.76^{c} ±0.05
D	98.61^{b} ±0.03	98.45^{c} ±0.18
E	94.32^{a} ±0.23	95.69^{c} ±0.58

Same letters between lines indicate no significant difference. Significance level $2\alpha = 0.05$.

matrix and causes lower retention; which differ from the results obtained in this study, since the active principle had a water-soluble character like the wall materials.

Although it is accepted that microencapsulation efficiency is affected positively by smaller droplet size (Holgado *et al*., 2013), in the current work the effect of the particle size on the %EE was not clear, given the freeze-dried formulation A after 1 and 2 microfluidization cycles (A_{FD1} and A_{FD2}) presented the lowest particle size and the lowest %EE; the semi-crystalline structure of MD10, then, could influence such results. Furthermore, it is possible that the highest particle size, presented by formulation E after 1 microfluidization cycle, could influence the %EE of sample E_{FD1}, although freeze-dried formulation B with an intermediate particle size after both cycles (B_{FD1} and B_{FD2}) did not present the optimum %EE. Nonetheless, %EE results agreed with Kausik and Roos (2007), who reported that emulsion droplet size did not affect the retention of limonene in freeze-drying, they attributed the retention by using different matrices with distinct characteristics; so that, the %EE of VE found in the current work could be attributed to the formulation, i.e. to the mixtures of MD20 and MD10 in certain ratios (90:10 and 95:05, respectively).

With respect to the X-ray analysis, the existence of some crystallinity degree could affect the retention of VE in samples A_{FD1} and A_{FD2}; the X-ray pattern that showed the semicrystalline nature of A samples could explain the lower value of %EE in both samples. In the case of samples B_{FD1} and B_{FD2}, it is important to point that, through DSC analysis, it was observed that MD10, was able to confer some crystallinity degree due to the amount present in B samples and, as a consequence, the %EE was reduced, which might be associated as well with the relatively high droplet size in the dispersion that originated the B-samples microcapsules.

Excepting sample A_{FD2}, the %EE results obtained in the current work were actually high (90%) enough to confirm the important presence of VE entrapped in the maltodextrins matrix which points out the effectiveness of the process and the formulations selected to encapsulate such active principle, and also to confirm the observations performed by CLSM. Moreover, it was interesting that the samples with a homogeneous distribution of VE inside the wall material (C_{FD1}, C_{FD2}, D_{FD1} and D_{FD2}) reported also the highest %EE. The release of VE from the semicrystalline structure of MD10 (samples A) during the freezing stage could explain the absence of the VE fluorescent signal on the surface layers of the microcapsules as showed the images obtained by the CLSM, because an active principle may be lost by vacuum conditions of freeze-drying processing (Najifi *et al*., 2011).

With the addition of 5-10% (w/w) of MD10 to a formulation with MD20, MD20 avoided that crystallization process of MD10 impacted negatively the %EE, and at the same time the structure of samples C_{FD1}, C_{FD2}, D_{FD1} and D_{FD2} was reinforced by MD10. There was no significant difference of %EE between samples A_{FD1} and E_{FD1}, which may be due to the formation of a semicrystalline structure (the former) and to a greater particle diameter (the latter).

Maltodextrins DE 10 and 20 are wall materials that have been used in several previous works on food products stabilization and encapsulation of flavor and bioactive compounds using freeze-drying for such purposes, for instance Che Man *et al*., (1999); Silva *et al*., (2005); Sánchez *et al*., (2013). In the cited works, all the entrapped materials had a hydrophilic nature and reported good results. In a similar way, the active principle studied here (vanilla extract) has a hydrophilic nature. The vanilla extract microcapsules obtained, as well, might work as a food ingredient, and maltodextrins would allow a faster redispersion and reduce the production cost. However, the markedly hydrophilic nature of MD20 could represent some long-term instability for the microcapsules, as well, the redispersed samples obtained with only MD10 show an opaque and cloudy appearance with traces of precipitate material. Given the above, the mixtures of maltodextrins would represent a good alternative as wall material for vanilla extract, but taking into account that MD20 must be the predominant compound in order to avoid complications for the subsequent redispersion tests. It was noticeable to observe how the drawback of one MD was covered with the advantage of the other. On one hand, while the higher affinity between MD20 and VE might limit the capability of the former to entrap the latter, the MD10 acted as a stabilizer of the MD20-VE interaction during the freeze-drying stage. On the other hand, while the higher viscosity, higher crystallinity and lower affinity between MD10 and VE might suggest the appropriate encapsulation of VE by MD10, the MD20 acted as an inhibitor of the MD10 crystallization which would make more difficult the microcapsule redispersion. Certainly, these effects are dependent on the MD20-MD10 ratio.

Conclusions

It was demonstrated the feasibility to conduct microencapsulation of a concentrated vanilla extract into a mixture of maltodextrins with different dextrose equivalent values through microfluidization followed by freeze-drying, in order to achieve high efficiency of encapsulation. The results have indicated that the predispersion of a mixture MD20:MD10 in 95:5 and 90:10 ratios after 2 microfluidization cycles and freeze-drying would produce microcapsules of vanilla extract with high encapsulation efficiency.

After considering, with especial importance, the solubility of the active principle and its affinity for each maltodextrin in the formulation, the differences in such dextrose equivalent were determinant in the viscosity and particle size of the formulations under study. However, the proportion in which the maltodextrins with different dextrose equivalent are present in the formulation constitutes a significant factor for determining the variations in crystallinity degree and the subsequent encapsulation efficiency achieved through the process performed here. Nevertheless, the effect of microfluidization pressure on droplet size distribution and microcapsule microstructure should be further studied.

Acknowledgements

Authors are grateful for the financial support of the Consejo Nacional de Ciencia y Tecnología (CONACYT) through doctoral scholarship. SIP projects 20151382, 20161380 and project SAGARPA-CONACyT 190442. Ocampo-Salinas is grateful for the financial support of CONACYT with register number 275972.

References

Adhikari, B., Howes, T., Sherestha, A. and Bhandari, B.R. (2007). Effect of surface tension and viscosity on the surface stickiness of carbohydrate and protein solution. *Journal of Food Engineering 79*, 1136-1143.

AOAC. (2005). *Methods of Analysis* (18th 375 ed.). Association of Official Analytical Chemist, Washington, D.C.

Avaltroni, F., Bouquerand, P. and Normand, V. (2004). Maltodextrin molecular weight distribution influence on the glass transition temperature and viscosity in aqueous solutions. *Carbohydrate Polymeres 58*, 323-334.

Baranauskiene, R., Bylaite, E., Zukauskaite, J. and Venskutonis, R.P. (2007). Flavor retention of peppermint (*Mentha piperita* L.) essential oil spray-dried in modified starches during encapsulation and storage. *Journal of Agricultral and Food Chemistry 55*, 3027-3036.

Biliaderis, C.G., Page, C.M., Maurice, T.J. and Juliano, B.O. (1986). Thermal Characterization of rice starches: a polymeric approach to phase transitions of granular starch. *Journal of Agricultral and Food Chemistry 34*, 6-14.

Bromiley, P. and Thacker, N. (2002). The effects of an arcsin square root transform on a binomial distributed quantity. *TINA memo*, 2002-2007.

Buera, P., Schebor, C., and Elizalde, B. (2005). Effects of carbohydrate crystallizatin on stability of dehydrated foods and ingredient formulations. *Journal of Food Engineering 67*, 157-165.

Cano-Sarmiento C., Monroy-Villagrana A., Alamilla-Beltrán L., Hernández-Sánchez H., Cornejo-Mazón M., Téllez-Medina D.I., Jiménez-Martínez C. and Gutiérrez-López G.F. (2014). Micromorphometric characteristics of α-tocopherol emulsions obtained by microfluidization. *Revista Meicana de Ineniería Química 13*, 201-212.

Che Man, Y., B., Irwandi, J. and Abdullah, W. J. (1999). Effect of different types of maltodextrins and drying methods on physic-chemical and sensory properties of encapsulated durian flavor. *Journal of the Science of Food and Agriculture 79*, 1075-1080.

Chetana, R., Krishnamurphy, S. and Yella Reddy, S. (2004). Rheological behavior of syrups containing sugar substitutes. *European Food Research and Technology 218*, 345-348.

Corveleyn, S. and Remon J.P. (1996). Maltodextrins as lyoprotectants in the lyophilization of a model protein, LDH. *Pharmaceutical Research 3*, 146-150.

da Costa, S.B., Duarte, C., Bourbon, A.I., Pinheiro, A.C., Serra, A.T., Martins, M.M., Januário, M.I.N., Vicente, A.A., Delgadillo, I. and

Duarte, C. (2012). Effect of the matrix system in the delivery and *in vitro* bioactivity of microencapsulated Oregano essential oil. *Journal of Food Engineering 110*, 190-199.

Dickinson, M.E., Bearman, G., Tille, S., Lansford, R. and Fraser, S.E. (2001). Multi-spectral imaging and linear unmixing add a whole new dimensions to laser scanning fluorescence microscopy. *Bioimaging 31*, 1272-1278.

Dokic, P., Jakovljevic, J. and Dokic-Baucal, L. (1998). Molecular characteristics of maltodextrins and rheological behavior of diluted and concentrated solutions. *Colloids and Surfaces A: Physicochemical and Engineering Aspects 141*, 435-440.

Dokic, L., Jakovljevic, J. and Dokic, P. (2004). Relation between viscous characteristics and dextrose equivalent of maltodextrins. *Starch-Stärke 56*, 520-525.

Domínguez-Hernández, C.R., García-Alvarado, M.A., García-Galindo, H.S., Salgado-Cervantes, M.A. and Beristain, C.I. (2016). Stability, antioxidant activity and bioavility of nano-emulsified astaxanthin. *Revista Mexicana de Ingeniería Química 15*, 457-468.

Fang, Z. and Bhandari, B. (2010). Encapsulation of polyphenols-a review. *Trends in Food Science and Technology 21*, 510-523.

Flores-Miranda, G.A., Valencia del Toro, G. and Yañes-Fernández. (2015). Stability Evaluation of ?carotene nanoemulsions prepared by homogenization-emulsification process using stearic acid as oil phase. *Revista Mexicana de Ingeniería Química 14*, 667-680.

Galmarini, M.V., Schebor, C., Zamora, M.C. and Chirife, J. (2009). The effect of trehalose, sucrose and maltodextrin addition on physicochemical and sensory aspects of freeze-dried strawberry puree. *International Journal of Food Science and Technology 44*, 1869-1876.

Goubet, I., Le Quere, J.-L. and Voilley, A. (1998). Retention of aroma compounds by carbohydrates: influence of their physicochemical characteristics and of their physical state. A review. *Journal of Agricultral and Food Chemistry 46*, 1981-1990.

Gu, F., Xu, F., Tan, L., Wu, H., Chu, Z. and Wang, Q. (2012). Optimization of enzymatic process for vanillin extraction using response surface methodology. *Molecules 17*, 8753-8761.

Harnkarnsujarit, N., Charoenrein, S. and Roos, Y.H. (2012). Microstructure formation of maltodextrin and sugar matrices in freeze-dried systems. *Carbohydrate Polymers 88*, 734-742.

Hernández-Hernández, H.M., Chanona-Pérez, J.J., Calderón-Domínguez, G., Perea-Flores, M.J., Mendoza-Pérez, J.A., Vega, A., Ligero, P., Palacios-González, E. and Farrera-Rebollo, R.R. (2014). Evaluation of agave fiber delignification by means of microscopy techniques and image analysis. *Microscoy and Microanalysis 20*, 1436-1446.

Hoffman, P.G. and Zapf C.M. (2011). Flavor, quality, and authentication, In: *Handbook of Vanilla Science and Technology*, Havkin-Frenkel, D. and Belanger, F. (Eds.). Blackwell Publishing, Ltd, UK, pp. 141-163.

Holgado, F., Marquez-Ruiz, G., Dobarganes, C. and Velasco, J. (2013). Influence of homogenization conditions and drying method on physicochemical properties of dehydrated emulsions containing different solid components. *International Journal of Food Science and Technology 48*, 1498-1508.

Jadeja, G., Maheshwari, R. and Naik, S. (2012). Pressurized liquid extraction of natural flavor from *Vanilla planifolia* Andrews. San Francisco, USA. 10th International Symposium on Supercritical Fluids.

Jafari, S.M., He, Y. and Bhandari, B. (2007a). Effectiveness of encapsulating biopolymers to produce sub-micron emulsions by high energy emulsification techniques. *Food Research International 40*, 862-873.

Jafari, S.M., He, Y. and Bhandari, B. (2007b). Optimization of nano-emulsions productions by microfluidization. *European Food Research and Technology 225*, 733-741.

Jeon, Y.-J., Vasanthan, T., Temelli, F. and Song, B.-K. (2003). The suitability of barley and corn starches in their native and chemically modified forms for volatile meat flavor encapsulation. *Food Research International 36*, 349-355.

Ji J., Zhang J., Chen J., Wang Y., Dong N., Hu C., Chen H., Li G., Pan X. and Wu C. (2015). Preparation and stabilization of a emulsions stabilized by mixed sodium caseinate and soy protein isolate. *Food Hydrocolloids 51*, 156-165.

Jun-xia, X., Hai-yan, Y. and Jian, Y. (2011). Microencapsulation of sweet orange oil by complex coacervation with soybean protein isolate/gum Arabic. *Food Chemistry 125*, 1267-1272.

Kaushik, V. and Roos, Y.H. (2007). Limonene encapsulation in freeze-drying of gum Arabic-sucrose-gelatin systems. *LWT- Food Science and Technology 40*, 1381-1391.

Liu, Y., Bhandari, B. and Zhou, W. (2006). Glass transition and enthalpy relaxation of amorphous food saccharides: a review. *Journal of Agricultral and Food Chemistry 54*, 5701-5717

Madene, A., Jacquot, M., Scher, J. and Desobry, S. (2006). Flavour encapsulation and controlled release - a review. *International Journal of Food Science and Technology 41*, 1-21.

Marcotte, M., Taherian Hoshahili, A.R. and Ramaswamy, H.S. (2001). Rheological properties of selected hydrcolloids as a function of concentration and temperature. *Food Research International 34*, 695-703.

Menczel, J.D., Judovits, L., Prime, R.B., Bair, H.E., Reading, M. and Swier, S. Differential scanning calorimetry (DSC). (2009). In: *Thermal analysis of polymers. Fundamentals and applications*. Menczel J.D and Prime R.B (Eds). Wiley and Sons publications. Nueva Jersey. EUA.

Milanovic, J., Manojlovic, V., Levic, S., Rajic, N., Nedovic, V. and Bugarski, B. (2010). Microencapsulation of flavors in carnauba wax. *Sensors 10*, 901-912.

Monroy-Villagrana A., Cano-Sarmiento C., Alamilla-Beltrán L., Hernández-Sánchez H. and Gutiérrez-López G.F. (2014). Coupled Taguchi-RSM optimization of the conditions to emulsify-tocopherol in an arabic gum-maltodextrin matrix by microfluidization. *Revista Mexicana de Ingeniería Químmica 13*, 679-688.

Najifi, M., Kadkhodace, R. y Mortazavi, S. (2011). Effect of drying process and wall material on the properties of encapsulated cardamom oil. *Food Biophysics 6*, 68-76.

Nielsen S. S. (2003). *Food Analysis*. 3rd. edition. Kluwer-Academic/Plenum Publishers. New York, USA. p. 503-541.

Nurhadi, B., Roos, Y. and Maidannyk, V. (2016). Physical properties of maltodextrin DE 10: water sortion, water plasticization and enthalpy relaxation. *Journal of Food Engineering 174*, 68-74.

Ocampo-Salinas I.O., Téllez-Medina D. I., Jiménez-Martínez C. and Dávila Ortiz G. (2016). Application of high pressure homogenization to improve satability and decrease droplet size in emulsion-flavor systems. *International Journal of Environment, Agriculture and Biotechnology 1*, 646-662.

Ochoa, A.A., Hernández-Becerra, J.A., Cavazos-Garduño, A., Vernon-Carter, E.J. and García, H.S. (2016). Preparation and characterization of curcumin nanoemulsions obtained by thin-film hydration emulsification and ultrasonication methods. *Revista Mexicana de Ingeniería Química 15*, 79-90.

Panagiotou, T., Bernard, M.J. and Mesite S.V. (2008). Deagglomeration and dispersion of carbon nanotubes using microfluidizer® high shear fluid processors. *NSTI-Nanotechnology 1*, 39-42.

Patravale, V.P., Date, A.A. and Kulkarni, R.M. (2004). Nanosuspension: a promising drug delivery strategy. *Journal of Pharmacy and Pharmacology 56*, 827-840.

Pérez, A., Sandoval, A.J., Cova, A. and Müller, A.J. (2014). Glass transitions and physical aging of cassava starch-corn oil blends. *Carbohydrate Polymers 105*, 244-252.

Qian, C. and McClements, D.J. (2011). Formation of nanoemulsions stabilized by model food-grade emulsifiers using high-pressure homogenization: factors affecting particle size. *Food Hydrocolloid 25*, 1000-1008.

Quintanilla-Carvajal, M.X., Meraz-Torres, L.S., Alamilla-Beltrán, L., Chanona-Pérez, J.J., Terres-Rojas, E., Hernández-Sánchez, H., Jiménez-Aparicio, A.R. and Gutiérrez-López, G.F. (2011). Morphmetric characerization of spary-dried microcapsules before and after-tocopherol extraction. *Revista Mexicana de Ingeniería Química 10*, 301-312.

Ranadive, A.S., (1992). Vanillin and related flavor compounds in vanilla extracts made from beans of various global origins. *Journal of Agricultral and Food Chemistry 40*, 1922-1924.

Ranadive, A.S. (2011). Quality control of vanilla beans and extracts, In: *Handbook of Vanilla Science and Technology*. Havkin-Frenkel D., Belanger, F. (Eds.), Blackwell Publishing, Ltd, UK, pp. 141-163.

Rodríguez, S.D., Wilderjans, T.F., Sosa, N. and Bernik, D.L. (2013). Image texture analysis and Gas sensor array studies applied to vanilla encapsulation by octenyl succinic anhydride starches *International Food Research 2*, 36.

Sánchez, V., Baeza, R., Galmarini, M.V., Zamora, M.C. and Chirife, J. (2013). Freeze-drying encapsulation of red wine polyphenols in an amorphous matrix of maltodextrin. *Food and Bioprocess Technology 6*, 1350-1354.

Sharma, A., Verma, S.C., Saxena, N., Chadda, N., Singh, N.P. and Sinha, A.K. (2006). Microwave and ultrasound assisted extraction of vanillin and its quantification by high?performance liquid chromatography in *Vanilla planifolia*. *Journal of Separation Science 29*, 613-619.

Sikora, M., Schilling, C.H., Tomasik, P. and Li, C. (2002). Dextrin plasticizers for aqueous colloidal processing of alumina. *Journal of the European Ceramic Society 22*, 626-628.

Silva, M., Sobral, P. and Kieckbusch T. (2005). State diagrams of freeze-dried camu-camu (*Myrciaria dubia* (HBK) Mc Vaugh) pulp with and without maltodextrin addition. *Journal of Food Engineering 77*, 426-422.

Sinha, A.K., Sharma, U.K. and Sharma, N. (2008). A comprehensive review on vanilla flavor: extraction, isolation and quantification of vanillin and others constituents. *International Journal of Food Sciences and Nutrition 59*, 299-326.

Siqueira, G., Bras, J. and Dufresne, A. (2010). Cellulosic Bionanocomposites: A review of preparation, properties and applicatins. *Polymers 2*, 728-765.

Soottitantawat, A., Bigeard, F., Yoshii, H., Furuta, T., Ohkawara, M. and Linko, P. (2005). Influence of emulsion and powder size on the stability of encapsulated D-limonene by spray drying. *Innovative Food Science and Emerging Technologies 6*, 107-114.

Sostaric, T., Boyce, M.C. and Spickett, E.E. (2000). Analysis of the volatile components in vanilla extracts and flavorings by solid-phase microextraction and gas chromatography. *Journal of Agricultral and Food Chemistry 48*, 5802-5807.

Tapia-Ochoategui, A., Camacho-Díaz, B., Perea-Flores, M., Ordonez-Ruiz, I., Gutiérrez-López, G., Dávila-Ortiz, G., (2011). Morfometric changes during the traditional curing process of vanilla pods (*Vanilla planifolia*; Orchidaceae) in Mexico. *Revista Mexicana de Ingeniería Química 10*, 105-115.

Udomrati, S., Ikeda, S. and Gohtani, S. (2013). Rheological properties and stability of oil-in-water emulsions containing tapioca maltodextrin in the aqeous phase. *Journal of Food Engineering 116*, 170-175.

Waliszewski, K.N., Pardio, V.T. and Ovando, S.L. (2007). A simple and rapid HPLC technique for vanillin determination in alcohol extract. *Food Chemistry 101*, 1059-1062.

Wang, S., Li, C., Copeland, L., Niu, Q. and Wang, S. (2015). Starch retrogradation: A comprehensive review. *Comprehensive Reviews in Food and Food Safety 14*, 568-585.

Wang, B., Wang, L.-j., Li, D., Wei, Q. and Adhikari, B. (2012). The rheological behavior of native and high-pressure homogenized waxy maize starch pastes. *Carbohydrate Polymers 88*, 481-489.

Wang, B., Wang, L., Li, D., Zhou, Y. and Özkan, N. (2011). Shear-Thickening properties of waxy maize starch dispersions. *Journal of Food Engineering 107*, 415-423.

Yang, Y., Marshall-Breton, C., Leser, M.E., Sher, A.A. and McClements, D.J. (2012). Fabrication of ultrafine edible emulsions: comparison of high-energy and low-energy homogenization methods. *Food Hydrocolloid 29*, 398-406.

Yang, Z., Peng, Z., Li, J., Li, S., Kong, L., Li, P. and Wang, Q. (2014). Development and evaluation of novel flavour microcapsules containing vanilla oil using complex coacervation approach. *Food Chemistry 145*, 272-277.

Zobel, H.F. (1964). X-ray analysis of starch granules. Page 109 in: *Methods in Carbohydrate Chemistry*. Vol. 4. R. L. Whistler, (ed.). Academic Press: Orlando, FL.